

Markus A. Wimmer,<sup>1</sup> Mathew T. Mathew,<sup>2</sup> Michel P. Laurent,<sup>2</sup>  
Christopher Nagelli,<sup>2</sup> Yifeng Liao,<sup>3</sup> Laurence D. Marks,<sup>3</sup>  
Robin Pourzal,<sup>2,4</sup> Alfons Fischer,<sup>2,4</sup> and Joshua J. Jacobs<sup>2</sup>

## Tribochemical Reactions in Metal-on-Metal Hip Joints Influence Wear and Corrosion

---

**REFERENCE:** Wimmer, Markus A., Mathew, Mathew T., Laurent, Michel P., Nagelli, Christopher, Liao, Yifeng, Marks, Laurence D., Pourzal, Robin, Fischer, Alfons, and Jacobs, Joshua J., "Tribochemical Reactions in Metal-on-Metal Hip Joints Influence Wear and Corrosion," *Metal-On-Metal Total Hip Replacement Devices* on May 8, 2012 in Phoenix, AZ; STP 1560, Steven M. Kurtz, A. Seth Greenwald, William M. Mihalko, and Jack E. Lemons, Editors, pp. 1–18, doi:10.1520/STP156020120050, ASTM International, West Conshohocken, PA 2013.

**ABSTRACT:** Recent findings indicate the presence of tribochemically generated layers on metal-on-metal (MoM) bearing surfaces. These tribolayers are films of a few-hundred-nanometer thickness and are constituted of carbonaceous material mixed with metal and oxide particles. The purpose of the study was to characterize these tribofilms mechanically and electrochemically. Using a nanoindenter, the local mechanical properties of the tribolayer were measured. On average a hardness of ~1.0 GPa was determined, which was softer than the underlying metal. The influence of tribomaterial on the electrochemistry of the cobalt–chromium–molybdenum alloy (CoCrMo) was investigated. Bovine calf serum mixture was used as the electrolyte. High- and low-carbon CoCrMo-samples with and without tribolayer were compared using potentiodynamic testing. This corrosive investigation was followed by tribocorrosive tests using a custom made apparatus, where a ceramic ball

---

Manuscript received May 23, 2012; accepted for publication September 5, 2012; published online April 10, 2013.

<sup>1</sup>Dept. of Orthopedic Surgery, Rush Univ. Medical Center, Orthopedic Building, 1611 W. Harrison St., Suite 204, Chicago, IL 60612, United States of America (Corresponding author), e-mail: [markus\\_a\\_wimmer@rush.edu](mailto:markus_a_wimmer@rush.edu)

<sup>2</sup>Dept. of Orthopedic Surgery, Rush Univ. Medical Center, Chicago, IL 60612, United States of America.

<sup>3</sup>Dept. of Materials Science and Engineering, Northwestern Univ., Evanston, IL 60201, United States of America.

<sup>4</sup>Materials Science and Engineering, Univ. of Duisburg-Essen, 47057 Duisburg, Germany.

oscillated against a flat CoCrMo surface. Potential and coefficient of friction were monitored throughout this 100 K cycle test. Electrochemical impedance spectroscopy tests before and after testing were conducted. Weight loss was determined using planimetric analysis. It was found that the tribolayered surface had better corrosion resistance than the corresponding tribolayer-free (polished) surface. The tribolayered surface also exhibited a more noble potential during tribocorrosive testing and demonstrated less wear. High-carbon was the superior alloy compared with low carbon for all surface conditions; however, the differences seemed to equalize in the presence of a tribofilm. There were also differences in tribofilm generation, possibly related to the microstructure of the two alloys.

**KEYWORDS:** tribochemical reactions, corrosion, tribocorrosion, tribofilms, wear

## Introduction

Considering all-metal bearings, tribochemical reactions can alter distinctively the chemical properties of surfaces. Typically, tribochemical reactions are essential for tribosystems running under boundary or mixed lubrication conditions. The reaction products hinder direct metal contact between the surfaces, and thus prevent the possibility of adhesion [1]. Tribochemical reactions lead to “tribofilms,” which have been observed in orthopedic all-metal joints by several authors dating back to the 1970s [2–7]. But only recently, the consequences with respect to wear sequence and interaction of wear mechanisms have been discussed and are further investigated.

Thus, it has been found that directly at the contact surface of cobalt–chromium–molybdenum (CoCrMo) hip balls or cups, nanocrystals as small as 10–70 nm are generated [8,9]. These nanocrystals are formed by a sequence of subsurface cyclic creep [10] caused by the introduction of alternating frictional shear stresses some  $\mu\text{m}$  below the surface and severe plastic deformation directly (some hundred nanometers) at the contact surface. Because the low stacking fault energy of CoCrMo alloys hinders the formation of dislocation cells (which would initiate fatigue cracks some  $\mu\text{m}$  below the surface), the nanocrystalline surface is supported sufficiently and can accommodate the high shear rates in contact. This nanocrystalline surface zone, is altered by carbonaceous material from the surrounding lubricant, which is incorporated up to a depth of 150 nm, most likely because of a mechanism, which has been called “mechanical mixing” [11]. Thus, some sort of nanocrystalline metallo-organic compound is generated as the actual contact material [12–14]. Once it is formed, it shows excellent tribological properties as suggested by the low steady-state wear rates after running-in. There is also evidence that graphitic material is present in such tribofilms, which would further explain their excellent tribological properties [15]. Whereas the mechanism of how the graphitic material forms is unknown, it appears that the proteins in the lubricant and their attachment to the surfaces could play a critical role. Catalytic reactions may

occur where the released metal assists in removing water from proteins leaving a hydrogenated carbon film. Further sliding on this film may lead to graphitic material. As graphite lowers the coefficient of friction under wet contact conditions, its presence on metal-on-metal hip components may help to keep the break-away torque low [14], and assist in generating low wear rates—also in the absence of a hydrodynamic fluid film.

This paper adds to the already existing morphological description of the tribofilm (or tribolayer) [12,14,15] with mechanical and electrochemical investigations. In particular, we have (a) studied the local mechanical properties of the tribofilm; and (b) demonstrated that the presence of a tribofilm beneficially affects the corrosion and tribocorrosion behavior of the cobalt-chromium alloy. For the study of tribocorrosion, we have employed techniques that recently emerged and appear helpful for the evaluation of the behavior of surfaces in mechanical contact in a chemically active environment [16–20].

## Materials and Methods

### *Evaluation of Nano-Hardness*

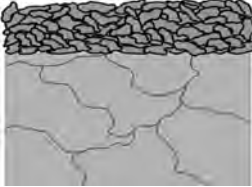
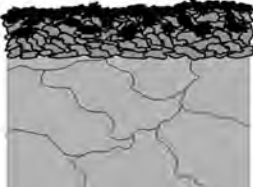
The hardness of the tribofilm was studied on a 42-mm-diameter ball of a retrieved hip surface replacement (ASR, DePuy Orthopaedics). It had been utilized by a female patient weighing 58 kg (body-mass index of 25.1 kg/m<sup>2</sup>) and was removed after 604 days in service. Using a Hysitron nanoindenter equipped with a Berkovich-type diamond tip, the tribofilm was indented with different loads ranging from 30 to 100  $\mu$ N. This was done to determine if the results are affected by applied load. The indentation depth was smaller than the tribofilm thickness.

The nano-hardnesses of the metallic matrix and alloy hard phases were measured for comparison. For this purpose, the alloy was cut and mechanically polished to mirror finish. The surface was then etched using a solution of 50 ml water + 50 ml HCl + 4g K<sub>2</sub>S<sub>2</sub>O<sub>5</sub> for 30 s. The applied load for nano-indentation was set to 4 mN. Any indentations located at phase or grain boundaries were discarded. The average hardness and standard deviation are reported.

### *Corrosion and Tribocorrosion Behavior of the Tribofilm*

*Sample Preparation*—Cylindrical pins were machined from rods of CoCrMo wrought alloy (ATI Allvac, USA). The pins were 12 mm in diameter and 7 mm in thickness with specification according to ASTM Standard 1714 [21]. In this study, two types of surface conditions were employed, polished, and tribolayered surfaces (Table 1), and these surface conditions were

TABLE 1—Overview of surface conditions in study.

Surface Condition	Polished	Tribolayered
Represents	Bearing surface without carbonaceous material	Bearing surface with carbonaceous material
Method of preparation	Mechanically polished	Mechanically polished with BCS as a lubricant
Schematic		

evaluated on high- (HC) and low-carbon- (LC) containing alloys (Table 2). The following preparation protocols were used:

- (i) **Polished:** The flat surface of the pin was mechanically polished to a mirror finish using traditional metallographic methods. The final polishing step implemented 1- $\mu\text{m}$  diamond paste to achieve a smoothness representative of a manufactured and finished implant ( $R_a < 0.04 \mu\text{m}$ ). The resulting nanostructure at or below the surface was less than 50 nm. The resulting nanocrystalline structure was in the range of what is seen in the primary contact area of a MoM hip implants (40 to 80 nm).
- (ii) **Tribofilm:** The surfaces of those samples were generated using the same standard metallographic polishing methods as described above, with a difference that a protein containing polishing lubricant was used. 1  $\mu\text{m}$  diamond paste mixed into bovine calf serum (BCS, 30 g/L protein) (see Table 3). The aim was to achieve a tribofilm formation that is comparable in appearance to those observed previously by Wimmer et al. [13,14]. Polishing was performed with a half automated polisher (LaboPol-1, Struers, Ballerup, Denmark). The polishing fluid was added in circular flow with a flexible tube

TABLE 2—Elemental composition of high and low-carbon wrought CoCrMo alloy of study.

	Diameter (mm)	Thickness (mm)	Chemical Composition (% wt.)						
			C	Co	Cr	Mo	Si	Mn	Al
High-carbon CoCrMo	29	7	0.241	64.60	27.63	6.04	0.66	0.70	0.02
Low-carbon CoCrMo	29	7	0.034	64.96	27.56	5.70	0.38	0.60	<0.02

TABLE 3—Composition of bovine calf serum lubricant and electrolyte.

NaCl (g/L)	EDTA (g/l)	Tris (g/l)	Protein (g/l)
9	0.2	27	30

pump. The applied force was  $18 \pm 3$  N. A tribofilm with embedded carbonaceous material was achieved after 6 h of processing. This film resembled features within the primary contact area of a MoM hip implant by visual and microscopic examinations

Six test samples per condition (alloy type and surface condition) were prepared and randomly assigned to corrosion and tribocorrosion testing ( $n = 3$  each). Before testing, all samples were washed in an ultrasonic cleaner for 10-min intervals in deionized water, and subsequently in 70 % isopropanol. Surfaces were dried in ambient air using a blow dryer.

*Corrosion Test*—The corrosion tests were conducted in a three-electrode electrochemical cell as per ASTM standard G61-86 [22]. The exposed area of the CoCrMo alloy ( $0.38 \text{ cm}^2$ ), a graphite rod and a calomel electrode (SCE) represented the working electrode, counter electrode and reference electrode, respectively. A total volume of 150 ml of BCS lubricant (30 g/L protein concentration) was used as an electrolyte for each experiment while the temperature was maintained at  $37^\circ\text{C} \pm 2^\circ\text{C}$ . The composition of BCS is provided in Table 3.

A custom protocol was developed to standardize the electrochemical tests. Initially, the open circuit potential (OCP) was monitored for a period of 1 h, and the system was allowed to stabilize electrochemically. The samples were then anodically polarized during the cyclic potentiodynamic test from  $-0.8 \text{ V}$  to  $+1.8 \text{ V}$  at a scanning rate of  $2 \text{ mV/s}$ . The corrosion parameters ( $I_{\text{corr}}$  - corrosion current density,  $E_{\text{corr}}$  - corrosion potential) were obtained from the potentiodynamic curves using Tafel's extrapolation method.

*Tribocorrosion Tests*—Tribocorrosion tests were conducted in a custom-made flat-on-ball apparatus that incorporated an electrochemical cell with a three-electrode system. Analogous to the corrosion tests, the three-electrode system of a working, auxiliary and reference electrode consisted of the exposed CoCrMo pin, graphite rod and calomel electrode (SCE). Also here a total volume of 150 ml of BCS was used as the lubricant/electrolyte. Each pin was loaded against a ceramic head oscillating  $\pm 15^\circ$  at 1 Hz for 100 K cycles. A schematic of the tribocorrosion setup is presented in Fig. 1 [20].

The test protocol included: (1) an initial stabilization period where a potential of  $-900 \text{ mV}$  was applied across the sample surface to “clean” the surface of any dirt or oxide layer, followed by an OCP period of 1 h to stabilize the system; (2) electrochemical impedance spectroscopy (EIS) was then applied to

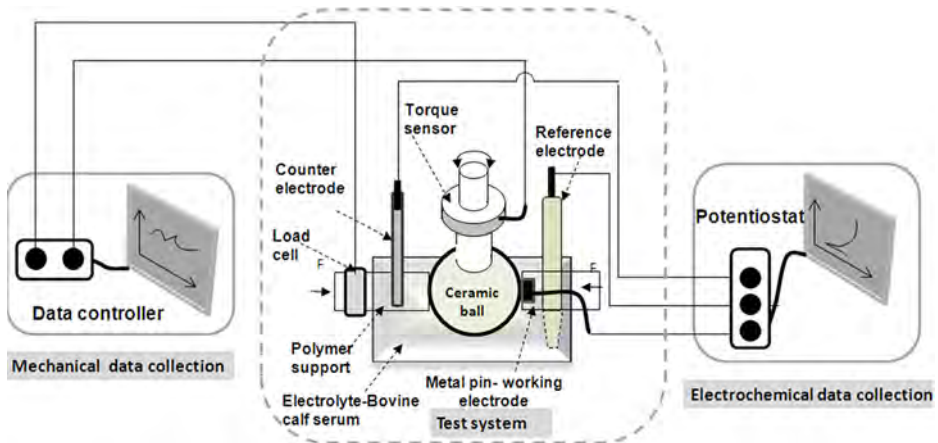


FIG. 1—*Experimental setup for tribocorrosion testing mainly consists of three components: (i) test system, (ii) mechanical data collection, and (iii) electrochemical data collection).*

characterize the electrochemical properties of the surface; (3) subsequently, the free potential during sliding was monitored along with the friction coefficient between the ceramic ball and pin surface; (4) EIS was applied again upon completion of the sliding experiment; and the system was then allowed to stabilize and the OCP was monitored during this period. Loss of material was determined by 3D profilometry and confirmed measuring the metal content in the lubricant as described earlier [5,23]. The testing protocol is illustrated in Fig. 2.

The EIS measurements were performed in the frequency range from 100 kHz to 0.01 Hz, with AC sine wave amplitude of 10 mV applied to the electrode at the corrosion potential ( $E_{\text{corr}}$ ).  $E_{\text{corr}}$  values are measured before the EIS test. For EIS data simulation, Zview2 software was used and a simple Randle's circuit composed of electrolyte resistance ( $R_s$ ) in series with a constant phase element (CPE) and in parallel with the polarization resistance ( $R_p$ ) was modeled. The impedance of a CPE is defined by  $Z_{\text{CPE}} = 1/((j\omega)^n C)$ , where

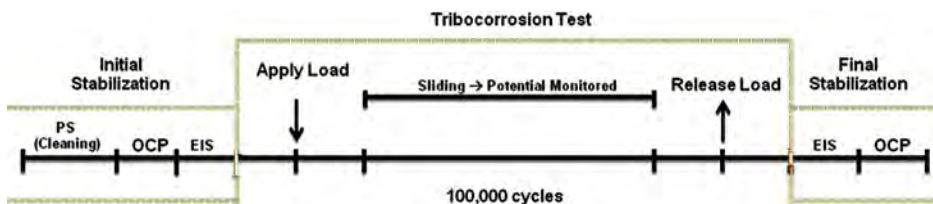


FIG. 2—*Tribocorrosion test protocol timeline (PS, potentiostatic; OCP, open circuit potential; EIS, electrochemical impedance spectroscopy).*

$j = (-1)^{1/2}$ ,  $w = 2\pi f$ , and the exponent “ $n$ ” of the CPE is related to non-equilibrium current distribution caused by surface roughness [24,25]. The parameter “ $C$ ” is a constant, representing true capacitance of the oxide barrier layer. Typically, better corrosion kinetics are obtained with high polarization resistance and low capacitance values [26]. However, this is a general rule which could be easily changed because of the complexity of the system. Three test replicas ( $n = 3$ ) were averaged and plotted as the ratio for “after/before” tribocorrosive testing. Profilometry measurements of the wear scar were performed using white light interferometry (Zygo New View 6300, Middlefield, CT, USA).

*Surface Characterization*—After testing, the samples were once again cleaned using the same procedure described previously. Typical collection times were 30 s and the accumulation of several measurements per sample are reported. Sample surfaces were also characterized by a white light interferometer (Zygo Corp., USA) for surface morphology and a scanning electron microscope (SEM) (JSM-5600 model, JOEL Co., Japan) for surface topography.

## Results

### *Nanohardness*

The hardness of the tribofilm adhering to the metallic substrate was determined to  $1.00 \pm 0.31$  GPa for an applied load of  $50 \mu\text{N}$ . The value was independent of applied load as can be seen in Table 4. The hardness values of the metallic matrix and hard phases were  $6.4 \pm 0.3$  GPa and  $15.9 \pm 0.9$  GPa, respectively.

### *Corrosion and Tribocorrosion Measurements*

*Polarization Curves and Corrosion Kinetics*—Polarization curves obtained from the corrosion tests are shown in Fig. 3. Figure 3(a) represents the HC-polished and tribolayered surfaces and 3(b) represent LC-polished and tribolayered surfaces. Although the general behavior was similar, the corrosion kinetics were not alike. In the case of HC, the tribolayered surface shows better passivation behavior than the polished surface, which is quite different from the LC surfaces.

TABLE 4—*Nanohardness of tribofilm measured under various applied loads.*

Force ( $\mu\text{N}$ )	30	50	70	100
Hardness (GPa)	$1.04 \pm 0.14$	$1.00 \pm 0.31$	$0.87 \pm 0.23$	$0.96 \pm 0.20$
Measurement No.	4	13	3	4

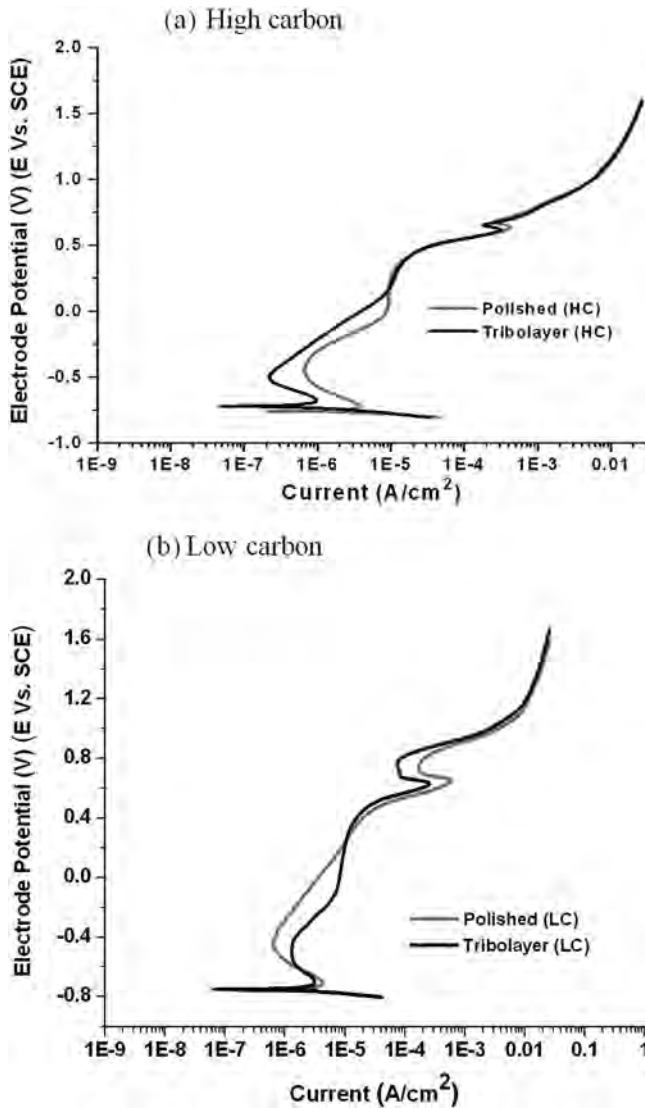


FIG. 3—Polarization curves—polished (HC and LC) and tribolayer: (a) high carbon (HC), and (b) low carbon (LC).

The Tafel parameters ( $E_{\text{corr}}$ ,  $I_{\text{corr}}$ ) describe the basic corrosion behavior of the exposed surface and the  $E_{\text{corr}}$  and  $I_{\text{corr}}$  values for the different surfaces are shown in Table 5. In general, a more cathodic  $E_{\text{corr}}$  value indicates a higher oxidation or corrosion tendency. No significant differences were observed for  $E_{\text{corr}}$ , neither between alloys, nor surface conditions (polished or tribolayered).

TABLE 5—*Electrochemical parameters (corrosion potential ( $E_{\text{corr}}$  (V)) and corrosion current ( $I_{\text{corr}}$  ( $\mu\text{A}$ )) estimated from polarization curves through Tafel's method.*

Material	Parameters	
	Corrosion Potential $E_{\text{corr}}$ (V)	Corrosion Current $I_{\text{corr}}$ ( $\mu\text{A}$ )
HC-polished	$-0.751 \pm 0.011$	$1.86 \pm 0.21$
LC-polished	$-0.741 \pm 0.013$	$2.49 \pm 0.46$
HC-tribolayer	$-0.729 \pm 0.011$	$0.76 \pm 0.09$
LC-tribolayer	$-0.729 \pm 0.018$	$0.77 \pm 0.17$

However, the tribolayered surfaces exhibited lower  $I_{\text{corr}}$  values when compared to the polished surface.

*Evolution of Potential and Friction Coefficient*—Evolution of potential and friction coefficient are presented as a function of sliding time, in Fig. 4 including: (a) for the HC-polished and tribolayered surface, and (b) for LC-polished and tribolayered surfaces. In both cases, a more noble potential was achieved in the presence of a tribofilm; however, the HC- alloy, showed a superior potential that was clearly evident. There was also a slight reduction of the friction coefficient for both alloys in the presence of a tribofilm,

*Weight Loss*—Weight loss calculations from tribocorrosion testing are shown in Fig. 5. Considering each surface condition, polished and tribolayered, HC demonstrated less wear than LC. Both alloys exhibited wear reduction in the presence of an existing tribofilm, which was more pronounced for the LC-alloy.

*Polarization Resistance and Double Layer Capacitance*— $R_p$  and  $C_{dl}$  ratios are shown in Fig. 6. There was a nearly fourfold increase of  $R_p$  for the HC-polished samples, which was topped by 16-fold increase of the LC-polished samples. The increases of the  $R_p$  for the tribolayered surfaces was low (HC) to non-existing (LC). Similarly, the capacitance changed. In this situation, the biggest changes occurred for the tribolayered surfaces (again with HC demonstrating the biggest improvement with regard to corrosion resistance). The HC-polished surface showed little to no change, whereas the  $C_{dl}$  ratio increased for the LC-polished surface.

*Surface Characteristics*—After 100 K the wear scar on the pin surface has the shape of a dimple because of the penetration of the ceramic ball. The wear patterns were relatively uniform within the entire wear scar with slightly more severe wear features at the center. SEM images of the wear patterns in the center of each wear scar are shown in Fig. 7(a)–7(d). In the case of the initially

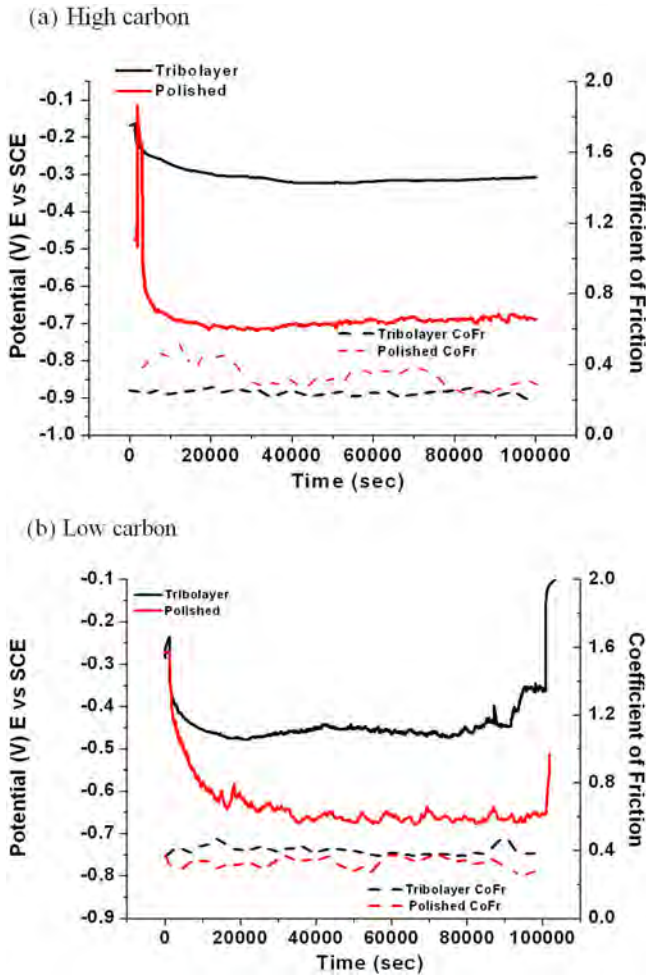


FIG. 4—Evolution potential and friction coefficient: (a) HC—polished and tribolayered, and (b) LC—polished and tribolayered.

polished LC CoCrMo alloy pin, patches of a carbonaceous film were observed (Fig. 7(a)). It appears that plastic deformation and wear resulted in a leveling of surface asperities. Figure 7(b) shows the wear pattern of the initially polished HC alloy CoCrMo pin. The surface, where sliding took place, clearly exhibits remains of a tribofilm. This layer appears to reside in surface depressions along with wear debris. Within the actual contact area it appears to be strongly adhering to the surface; however, because of numerous scratches with random orientation this tribolayer looks disrupted. The surfaces of either alloy exhibited relatively uniform tribofilms after 100 K cycles with a similar appearance as those reported earlier in all-metal hip replacements [6]. As illustrated

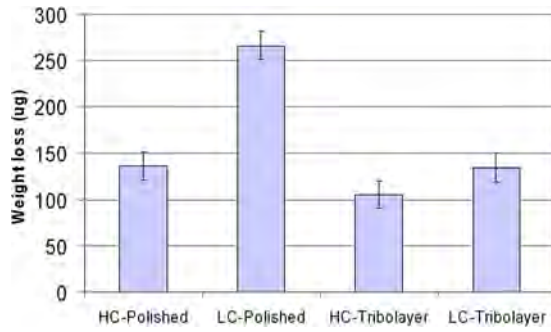


FIG. 5—Weight loss—(FP) polished (HC and LC), and tribolayer (HC and LC).

in Figs. 7(c) and 7(d) there was no significant difference between LC and HC CoCrMo alloy. In both cases, random scratches were apparent in which the tribolayer was removed.

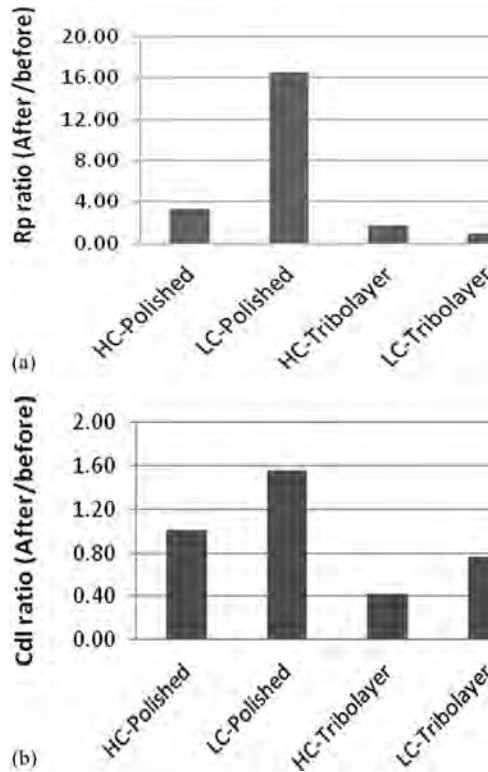


FIG. 6—Ratios of EIS parameters: (a) polarization resistance ( $R_p$ ) (after/before), and (b) double layer capacitance (after/before).

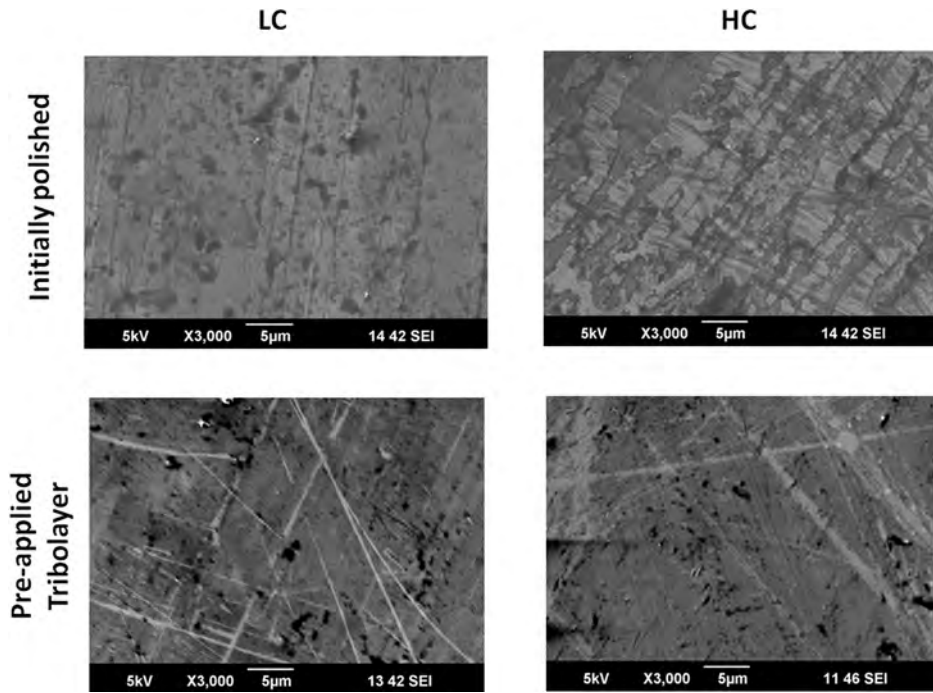


FIG. 7—SEM images of the worn surfaces after the tribocorrosion tests (free potential): (a) LC-polished, (b) HC-polished, (c) LC-tribolayer, and (d) HC-tribolayer.

## Discussion

This study focused on the effects of tribochemical reactions in MoM hip joints. In vivo, tribochemical reactions between metal and surrounding synovial fluid result in the generation of a metallo-organic composite at the surface. This layer has been referred to as “tribofilm” or “tribolayer” to underscore that structure and composition are different from the base material [12,13]. More recently, it has been shown that the film contains graphitic material suggesting distinct triboactive properties for the mixed or boundary lubrication mode [15]. The presence of such a tribofilm may help to stabilize the ultra-mild wear regime of MoM bearings in the absence of a fluid film. To better understand the mechanical interaction of the tribofilm with the countersurface, we measured the hardness of the film. As expected the tribofilm was softer than the CoCrMo metal matrix (and any other constituent), although it is worth noting that the tribofilm measurements may have been influenced by the hardness of the underlying matrix. This suggests that the film may increase the contact area (thus lowering contact stresses) under applied load. The softness of the film might be linked to a low shear modulus helping to dissipate the introduced energy and act as a lubricant during articulation.

There have been some indications that the tribofilm should improve the wear behavior of metallic articulation, however it is unknown if the corrosive and tribocorrosive properties of LC and HC-alloys change in the presence of a tribofilm. Such questions are being addressed using an electrochemical approach with a standard three electrode corrosion cell and an attached potentiostat [19]. Recently, Igual Muñoz and Mischler [27] investigated the interaction of albumin and phosphates present in the body fluids on the passivation behavior of CoCrMo alloys. The study revealed that phosphates and proteins play a significant role in the electrochemical properties of the metal/oxide/electrolyte interface, which influences the corrosion kinetics. Our own results demonstrated that physiological conditions (simulated with bovine calf serum) improve the passivation kinetics of the CoCrMo alloy, as follows.

The polarization curves for the polished HC and LC alloy samples were surprisingly similar and there was little distinction in electrochemical behavior. However, there was a significant difference in corrosion mechanisms and passivation kinetics for the tribolayered HC and LC surfaces, which appears to be related to elemental composition and microstructure of the alloys [28]. Overall, the tribolayered surfaces demonstrated a better corrosion behavior than the polished surfaces, as primarily reflected by the  $I_{\text{corr}}$  values. The lower  $I_{\text{corr}}$  values obtained for the tribolayered samples suggest corrosion inhibiting characteristics of the tribofilm [29–31]. Because the  $E_{\text{corr}}$  is a measure of corrosion tendency the similarity in  $E_{\text{corr}}$  values indicates that the electron transfer affinity has not changed between the polished and tribolayered surfaces. In summary, it can be stated that the difference in carbon content between the HC and the LC alloy did not affect the  $I_{\text{corr}}$  behavior, whereas the variation in surface condition did.

In the wear experiment, a smaller weight loss was found under free potential conditions for the HC alloy compared to the LC alloy, whether polished or tribolayered. This is consistent with the reported wear performance of the high carbon alloy both in both pin-on-flat and pin-on-disk wear tests [32–34] and hip simulator tests [35]. However, the difference between the HC and LC alloys is much higher when the initial surface is as-polished than when it is tribolayered, consistent with a protective effect of the tribolayer under the present test conditions. The polished LC alloy demonstrated the largest increase in the polarization resistance (16-fold, Fig. 6), suggesting that it is the more susceptible to the effect of a tribolayer and that most of the weight loss for this alloy in the polished state was from running-in wear, as the tribolayer was being formed. The higher corrosion current for the LC alloy (Fig. 4) compared to the HC alloy may favor the formation of a tribolayer by releasing a larger number of metal ions. These ions can react with the proteins in the lubricant to denature them [36,37] and thus enhance the deposition of a proteinaceous film. The film is then converted to the tribolayer through further tribochemical reactions and mixing with the nanocrystalline layer of the metallic surface [13]. The

after/before sliding ratio of the double layer capacitance,  $C_{dl}$  (Fig. 6(b)) closely correlated with weight loss (Fig. 5) for the four conditions studied. Because an increase in  $C_{dl}$  is usually associated with greater electrochemical reactivity [38,39], this correlation suggests that the wear and corrosion processes are closely connected through a tribocorrosive synergism, meaning that the re-passivation kinetics, as well as the structure and mechanical nature of the reformed oxide layer are dependent on each other.

The above observations are consistent with the wear features observed after testing. The SEM images of initially polished samples clearly show that running-in was not entirely completed. This was represented by the surface alterations for the LC samples including surface asperities and depressions, as well as numerous scratches of the HC samples. Such surface depressions may be caused by hard phases (e.g., carbides) breaking out of the surface during running-in and subsequently introducing three-body wear as has been described numerous times in the literature [e.g., 40]. Interestingly, when initially tribolayered, both alloys exhibited mild wear features. Again, this suggests that a tribofilm reduces wear. Also, it appears that once a tribofilm has formed, the carbon content of the alloy is no longer of significance, which was reflected in the tribocorrosion data.

It is worthwhile to reflect about the scope and the limitations of the study. This study focused on tribochemical reactions and the generation of tribofilms in MoM bearings. Based on the findings of this study, it appears that the tribofilm has beneficial tribocorrosive effects, thereby reducing particle and ion release. However, cause and effect are not fully determined. It is possible that the initial wear-in is a prerequisite for the formation of tribolayer. Wearing-in results in a higher conformity of the articulation with enhanced fluid film separation, and thus low wear rates. Further, the study is limited in several technical aspects. A ceramic rather than a metallic ball was used to articulate against the pin. This was done in an attempt to electrically isolate the pin from the ball and allow precise electrochemical measurements. A flat rather than a conforming pin surface was used, which lead to high running-in wear and continuously changing contact conditions. Also, the testing periods were rather short and wear may not have stabilized within the investigated interval. Nevertheless, based on the findings of this study, the following conclusions are drawn.

## Conclusions

- Tribochemical reactions lead to a surface anchored tribofilm in metal-on-metal joints.
- The alloy's microstructure (HC or LC) appears inherently involved in the generation of the tribofilm.
- The tribofilm is softer than the metal matrix allowing increased contact with the counterface.

- Surfaces with tribofilm demonstrate reduced current density at  $E_{\text{corr}}$ , which suggests increased corrosion resistance.
- Samples with tribofilm show less material removal during wear testing compared with polished surfaces.
- Generation of a carbonaceous film leads to an increase in polarization resistance of the surface, which further changes the double layer capacitance of the surface. The changes correlate with weight loss of the sample and this behavior suggests a close synergistic interaction of wear and corrosion.

### Acknowledgments

This study is funded by the National Institutes of Health (NIH) under Grant No. 1RC2AR058993. Special thanks go to Howard Freeze, ATI Allvac, for providing the cobalt–chrome alloys for this study.

### References

- [1] Zum Gahr, K. H., *Microstructure and Wear of Materials, Tribology Series*, Vol. 10, Elsevier, Amsterdam, 1987.
- [2] Walker, P. S., Salvati, E., and Hotzler, R. K., “The Wear on Removed McKee-Farrar Total Hip Prostheses,” *J. Bone Joint Surg. Am.*, Vol. 56, No. 1, 1974, pp. 92–100.
- [3] Semlitsch, M., Streicher, R. M., and Weber, H., “Verschleißverhalten von Pfannen und Kugeln aus CoCrMo-Gußlegierung bei langfristig implantierten Ganzmetall Hüftprothesen,” *Orthopäde*, Vol. 18, 1989, pp. 377–381.
- [4] McKellop, H., Park, S. H., Chiesa, R., Doorn, P., Lu, B., Normand, P., Grigoris, P., and Amstutz, H., “In Vivo Wear of Three Types of Metal on Metal Hip Prostheses During Two Decades of Use,” *Clin. Orthop. Relat. Res.*, Vol. 329 (Suppl.), 1996, pp. 128–140.
- [5] Wimmer, M. A., Loos, J., Nassutt, R., Heitkemper, M., and Fischer, A., “The Acting Wear Mechanisms on Metal-on-Metal Hip Joint Bearings—In Vitro Results,” *Wear*, Vol. 250, pp. 129–139.
- [6] Wimmer, M. A., Sprecher, C., Hauert, R., Tager, G., and Fischer, A., “Tribochemical Reaction on Metal-on-Metal Hip Joint Bearings: A Comparison Between In-Vitro and In-Vivo Results,” *Wear*, Vol. 255, 2003, pp. 1007–1014.
- [7] Burgette, M. D., Donaldson, T. K., and Clark, I. C., “Denatured Protein Deposits Identified on Simulator and Explants Hip Bearings,” Symposium on Metal-on-Metal Hip Replacement Devices ASTM F04, Phoenix, AZ, May 8, 2012, ASTM International, West Conshohocken, PA.

- [8] Büscher, R., Täger, G., Gleising, B., Dudzinski, W., Wimmer, M. A., and Fischer, A., "Subsurface Microstructure of Metal-on-Metal Hip Joints and Its Relationship to Wear Particle Generation," *J. Biomed. Mater. Res. B Appl. Biomater.*, Vol. 72B, No. 1, 2005, pp 206–214.
- [9] Büscher, R. and Fischer, A., "The Pathways of Dynamic Recrystallization in All-Metal Hip Joints," *Wear*, Vol. 259, Nos. 7–12, 2005, pp. 887–897.
- [10] Fischer, A., Weiss, S., and Wimmer, M. A., "The Tribological Difference between Biomedical Steels and CoCrMo-Alloys," *J. Mech. Behav. Biomed. Mater.*, Vol. 9, 2012, pp. 50–62.
- [11] Rigney, D. A., "Transfer, Mixing and Associated Chemical and Mechanical Processes During the Sliding of Ductile Materials," *Wear*, Vol. 245, 2000, pp. 1–9.
- [12] Pourzal, R., Theissmann, R., Williams, S., Gleising, B., Fisher, J., and Fischer, A., "Subsurface Changes of a MoM Hip Implant Below Different Contact Zones," *J. Mech. Behav. Biomed. Mater.*, Vol. 2, No. 2, 2009, pp. 186–191.
- [13] Wimmer, M. A., Fischer, A., Büscher, R., Pourzal, R., Sprecher, C., Hauert, R., and Jacobs, J. J., "Wear Mechanisms in Metal-on-Metal Bearings: The Importance of Tribochemical Reaction Layers," *J. Orthop. Res.*, Vol. 28, No. 4, 2010, pp. 436–443.
- [14] Wimmer, M. A., Nassutt, R., Sprecher, C., Loos, J., Täger, G., and Fischer, A., "Investigation on Stick Phenomena in Metal-on-Metal Hip Joints after Resting Periods," *Proc. Inst. Mech. Eng. H*, Vol. 220, 2006, pp. 219–227.
- [15] Liao, Y., Pourzal, R., Wimmer, M. A., Jacobs, J. J., Fischer, A., and Marks, L. D., "Graphitic Tribological Layers in Metal-on-Metal Hip Replacements," *Science*, Vol. 334, No. 6063, 2011, pp. 1687–1690.
- [16] Mischler, S., "Triboelectrochemical Techniques and Interpretation Methods in Tribocorrosion: A Comparative Evaluation," *Tribol. Int.*, Vol. 41, 2008, pp. 573–583.
- [17] Yan, Y., Neville, A., and Dowson, D., "Biotribocorrosion an Appraisal of the Time Dependence of Wear and Corrosion Interactions: I. The Role of Corrosion," *J. Phys. D: Appl. Phys.*, Vol. 39, 2006, p. 32.
- [18] Yan, Y., Neville, A., Dowson, D., and Williams, S., "Tribocorrosion in Implants—Assessing High Carbon and Low Carbon Co-Cr-Mo Alloys by in Situ Electrochemical Measurements," *Tribol. Int.*, Vol. 39, 2006, pp. 1509–1517.
- [19] Mathew, M. T., Srinivasa Pai, P., Pourzal, R., Fischer, A., and Wimmer, M. A., "Significance of Tribocorrosion in Biomedical Applications: Overview and Current Status," *Adv. Tribol.*, Vol. 2009, 2009, Article ID 250986.
- [20] Mathew, M. T., Runa, M. J., Laurent, M., Jacobs, J. J., Rocha, L. A., and Wimmer, M. A., "Tribocorrosion Behavior of CoCrMo Alloy for Hip

- Prosthesis as a Function of Loads: A Comparison Between Two Testing Systems,” *Wear*, Vol. 271, 2011, pp. 1210–1219.
- [21] ASTM 1714, 2002, “Wear of Prosthetic Hip Designs,” *Annual Book of ASTM Standards*, Vol. 13.01, ASTM International, West Conshohocken, PA.
- [22] ASTM G61-86, 2002, “Standard Test Method for Conducting Cyclic Potentiodynamic Polarization Measurements for Localized Corrosion Susceptibility of Iron-, Nickel-, or Cobalt-Based Alloys,” *Annual Book of ASTM Standards*, Vol. 03.02, ASTM International, West Conshohocken, PA.
- [23] Wimmer, M. A., Artelt, D., Schneider, E., Kunze, J., Morlock, M. M., and Nassutt, R., “Friction and Wear Properties of Metal/Metal Hip Joints,” *Mat.-wiss. u. Werkstofftech.*, Vol. 32, 2001, pp. 891–896.
- [24] Abdel-Rehim, S. S., Khaled, K. F., and Abd-Elshafi, N. S., “Electrochemical Frequency Modulation as a New Technique for Monitoring Corrosion Inhibition of Iron in Acid Media by New Thiourea Derivative,” *Electrochim. Acta*, Vol. 51, 2006, pp. 3269–3277.
- [25] Rehim, S. S. A., Hassan, H. H., and Amin, M. A., “Corrosion and Corrosion Inhibition of Al and Some Alloys in Sulphate Solutions Containing Halide Ions Investigated by an Impedance Technique,” *Appl. Surface Sci.*, Vol. 187, 2002, pp. 279–290.
- [26] Mathew, M. T., Barao, V., Yuan, J. C., Assunção, W. G., Cortino, S., and Wimmer, M. A., “What is the Role of Lipopolysaccharide on the Tribocorrosive Behavior of Titanium?” *J. Mech. Behav. Biomed. Mater.*, Vol. 8, 2011, pp. 71–85.
- [27] Igual Muñoz, A. and Mischler, S., “Interactive Effects of Albumin and Phosphate Ions on the Corrosion of CoCrMo Implant Alloy,” *J. Electrochem. Soc.*, Vol. 154, 2007, pp. 562–570.
- [28] Panigrahi, P., Liao, Y., Mathew, M. T., Nagelli, C., Fischer, A., Wimmer, M. A., and Marks, L. D., “Corrosion Behavior of Solution-Annealed CoCrMo Alloy for Metal-on-Metal (MoM) Hip Joint Application,” Poster No. 2068, *ORS 2012 Annual Meeting*, San Francisco, CA, Feb 4–7, Orthopaedic Research Society, Rosemont, IL.
- [29] Khan, M. A., Williams, R. L., and Williams, D. F., “In-Vitro Corrosion and Wear of Titanium Alloys in the Biological Environment,” *Biomaterials*, Vol. 17, 1996, pp. 2117–2126.
- [30] Khan, M. A., Williams, R. L., and Williams, D. F., “The Corrosion Behaviour of Ti–6Al–4V, Ti–6Al–7Nb and Ti–13Nb–13Zr in Protein Solutions,” *Biomaterials*, Vol. 20, 1999, pp. 631–637.
- [31] Williams, R. L., Brown, S. A., and Merritt, K., “Electrochemical Studies on the Influence of Proteins on the Corrosion of Implant Alloys,” *Biomaterials*, Vol. 9, 1988, pp. 181–186.
- [32] Scholes, S. C. and Unsworth, A., “Pin-on-Plate Studies on the Effect of Rotation on the Wear of Metal-on-Metal Samples,” *J. Mater. Sci. Mater. Med.*, Vol. 12, 2001, pp. 299–303.

- [33] Tipper, J. L., Firkins, P. J., and Ingham, E., "Quantitative Analysis of the Wear and Wear Debris From Low and High-Carbon Content Chrome Alloys Used in Metal-on-Metal Hip Replacements," *J. Mater. Sci. Mater. Med.*, Vol. 10, 1999, pp. 353–363.
- [34] St. John, K. R., Zardiackas, L. D., and Poggie, R. A., "Wear Evaluation of Cobalt-Chromium Alloy for Use in a Metal-on-Metal Hip Prosthesis," *J. Biomed. Mater. Res. B Appl. Biomater.*, Vol. 68, 2004, pp. 1–14.
- [35] St. John, K. R., Poggie, R. A., Zardiackas, L. D., and Afflitto, R. M., "Comparison of Two Cobalt-Based Alloys for Use in Metal-on-Metal Hip Prostheses: Evaluation of the Wear Properties in a Simulator," *Cobalt-Base Alloys for Biomedical Applications*, ASTM STP 1365, J. A. Disegi, R. L. Kennedy, and R. Pilliar, Eds., ASTM International, West Conshohocken, PA, 1999.
- [36] Borguet, F., Cornelis, R., Delanghe, J., Lambert, M. C., and Lameire, N., "Study of the Chromium Binding in Plasma of Patients on Continuous Ambulatory Peritonea l Dialysis," *Clin. Chim. Acta*, Vol. 238, 1995, pp. 71–84.
- [37] Meucci, E., Mordente, A., and Martorana, G. E., "Metal Catalyzed Oxidation of Human Serum Albumin—Conformational and Functional Changes and Implications in Protein Aging," *J. Biol. Chem.*, Vol. 266, 1991, pp. 4692–4699.
- [38] Mathew, M. T., Arizaa, E., Rochaa, L. A., Vazd, F., Fernandesd, A.C., and Stack, M. M., "Tribocorrosion Behaviour of TiCxOy Thin Films in Bio-Fluids," *Electrochim. Acta*, Vol. 56, 2010, pp. 929–937.
- [39] Ponthiaux, P., Wenger, F., Drees, D., and Celis, J. P., "Electrochemical Techniques for Studying Tribocorrosion Process," *Wear*, Vol. 256, 2004, pp. 459–468.
- [40] Park, S. H., McKellop, H., Lu, B., Chan, F., and Chiesa, R., "Wear Morphology of Metal–Metal Implants: Hip Simulator Tests Compared with Clinical Retrievals." *Alternative Bearing Surfaces in Total Joint Replacement*, STP 1346, ASTM International, 1998, pp. 129–143.